HHS Public Access

Author manuscript

Hear Res. Author manuscript; available in PMC 2018 March 01.

Published in final edited form as:

Hear Res. 2017 March ; 345: 10–22. doi:10.1016/j.heares.2016.12.012.

Culture media-based selection of endothelial cells, pericytes, and perivascular-resident macrophage-like melanocytes from the young mouse vestibular system

Dr. Jinhui Zhang [researcher fellow],
Oregon Hearing Research Center, Department of Otolaryngology / Head and Neck Surgery, Oregon Health & Science University, for the conduct of the study).

Dr. Songlin Chen [researcher fellow],
Oregon Hearing Research Center, Department of Otolaryngology / Head and Neck Surgery, Oregon Health & Science University, for the conduct of the study).

Dr. Jing Cai [researcher fellow],
Oregon Hearing Research Center, Department of Otolaryngology / Head and Neck Surgery, Oregon Health & Science University, for the conduct of the study).

Dr. Zhiqiang Hou [researcher fellow],
Oregon Hearing Research Center, Department of Otolaryngology / Head and Neck Surgery, Oregon Health & Science University, for the conduct of the study).

Dr. Xiaohan Wang [current researcher fellow],
Oregon Hearing Research Center, Department of Otolaryngology / Head and Neck Surgery, Oregon Health & Science University).

Dr. Allan Kachelmeier [current researcher fellow], and
Oregon Hearing Research Center, Department of Otolaryngology / Head and Neck Surgery, Oregon Health & Science University).

Xiaorui Shi, M.D., Ph.D.
Oregon Hearing Research Center, Department of Otolaryngology / Head and Neck Surgery, Oregon Health & Science University, Portland, OR 97239, Phone: 503 494-8032, Fax: 503 494-5656 / shix@ohsu.edu

Abstract

The vestibular blood-labyrinth barrier (BLB) is comprised of perivascular-resident macrophage-like melanocytes (PVM/Ms) and pericytes (PCs), in addition to endothelial cells (ECs) and basement membrane (BM), and bears strong resemblance to the cochlear BLB in the stria vascularis. Over the past few decades, *in vitro* cell-based models have been widely used in blood-brain barrier (BBB) and blood-retina barrier (BRB) research, and have proved to be powerful tools

(*All authors for the conduct of the study were and are at the same institute).

for studying cell-cell interactions in their respective organs. Study of both the vestibular and strial BLB has been limited by the unavailability of primary culture cells from these barriers. To better understand how barrier component cells interact in the vestibular system to control BLB function, we developed a novel culture medium–based method for obtaining EC, PC, and PVM/M primary cells from tiny explants of the semicircular canal, sacculus, utriculus, and ampullae tissue of young mouse ears at post-natal age 8 - 12 d. Each phenotype is grown in a specific culture medium which selectively supports the phenotype in a mixed population of vestibular cell types. The unwanted phenotypes do not survive passaging. The protocol does not require additional equipment or special enzyme treatment. The harvesting process takes less than 2 h. Primary cell types are generated within 7 - 10 d. The primary culture ECs, PCs, and PVM/M shave consistent phenotypes more than 90% pure after two passages (~ 3 weeks). The highly purified primary cell lines can be used for studying cell-cell interactions, barrier permeability, and angiogenesis.

Keywords

mouse cochlear vestibular system; blood-labyrinth barrier; primary cell culture; endothelial cell; pericyte; perivascular-resident macrophage-like melanocytes

1. Introduction

The blood-labyrinth barrier (BLB) in the vestibular system tightly regulates the vestibular microenvironment for functional balance and coordination (Rybak, 1995). Integrity of the barrier is critical for maintaining fluid ion homeostasis in the ear, a *sine quanon* for signal transduction and vestibular function. Disruption of the BLB has long been considered an etiologic factor in a variety of vestibular disorders, including Ménière's disease, and meningitis-associated labyrinthitis (Juhn et al., 2001; Laurell et al., 2008; Tagaya et al., 2011; Trune, 1997). Despite the importance of the BLB to vestibular function, mechanisms that control BLB barrier permeability remain largely unknown. Information on regulation of the BLB in the vestibular system is sparse.

The structure of the BLB in the vestibular system is similar to the BLB of the intra-strial fluid-blood barrier. At the cellular level, the BLB is comprised of cochlear microvascular endothelial cells (ECs) lining cochlear microvessels, associated basement membrane, and a “second line of component cells” including cochlear pericytes (PCs) and perivascular resident macrophage-like melanocytes (PVM/Ms) (Zhang et al., 2013). The BLB is formed by tight junctions (TJs) between the ECs, like other blood-tissue barriers, but the barrier is further characterized by its carrier-mediated transport system and absence of fenestration(Sakagami et al., 1986).

Over the past few decades, *in vitro* cell-based models are widely used in blood-brain-barrier (BBB) and blood-retina-barrier (BRB) studies. The cell line-based *in vitro* BBB or BRB models have proven to be powerful tools for studying cell-cell interactions and regulation of blood barrier permeability(Cucullo et al., 2002; Duport et al., 1998; Lai et al., 2005). However, these research tools have been of limited use in studying the BLB due to the difficulty of isolating BLB component cells from the vestibular system. Although different methods of isolation and culture of barrier cells from the brain, retina, skeletal muscle, skin,

and fetal tissues have been successfully used to obtain barrier component cells (Bryan et al., 2008; Crisan et al., 2008; Mogensen et al., 2011; Sundberg et al., 2002), most of the methods are time-consuming and involve multiple steps of enzymatic digestion, gradient density centrifuging, and glass bead or magnetic separation (Bowman et al., 1983; Bowman et al., 1981; Ohtsuki et al., 2007; Stins et al., 1997). The techniques are usually performed in non-cochlear tissues from rat (Ohtsuki et al., 2007), porcine (Mischeck et al., 1989), or bovine models (Ryan, 1984) where tissue volume is not limited(Ballarin et al., 2012; Leppens et al., 1996; Xie et al., 1997). However, the microvasculature in the vestibular system is small in volume and anatomically complex. These constraints have impeded the production of vestibular BLB component cells by commonly used capillary extraction and isolation methods. The difficulty in isolating BLB component cells has limited our understanding the functional role of each cell type in the BLB of the vestibular system.

In this study, we describe a novel method which uses a specifically formulated culture media to selectively grow EC, PC, and PVM/M phenotypes from fragmented young mouse vestibular tissue. The method was earlier developed for production of EC, PC and PVM/M phenotypes from cochlear strial tissue. The method is practicable and provides consistent results. Blood barrier component cells from different organs and tissues show organ and tissue specific differences (Garlanda et al., 1997; Invernici et al., 2005). Extrapolation of vestibular BLB function using non-vestibular barrier cell lines such as obtained from the cochlea, brain, and kidney may not accurately reflect the physiological features of the BLB. Primary cell lines generated directly from the BLB of the vestibular system enables us to investigate the specific role of each phenotype on BLB integrity and identify vestibular organ-specific characteristics of the BLB.

2. Materials and Methods

2.1 Animals

C57BL/6J mice, purchased from Jackson Laboratory (Bar Harbor, ME, USA), were inbred and used at age 8 –12 d. The protocol for the care and use of these animals was approved by the Institutional Animal Care and Use Committee at Oregon Health & Science University (the IACUC approval number is IS00003678).

2.2 Collection of vestibular end-organs from young mouse ears

The mice were anesthetized with ketamine hydrochloride (100 mg/kg, intramuscular) and 2% xylazine hydrochloride (10 mg/kg, Abbott Laboratories, USA). The auditory bullae was rapidly removed and placed in a Petri dish filled with cold, fresh artificial perilymph solution. The surgery was performed under sterile conditions. The vestibular sacculus, utriculus, and ampullae of the semicircular canal tissue were gently extracted and placed in a cold artificial perilymph solution containing 125 mmol/L NaCl, 3.5 mmol/L KCl, 1.3 mmol/L $CaCl_2$, 1.5 mmol/L $MgCl_2$, 0.51 mmol/L NaH_2PO4, 10 mmol/L Hepes, and 5 mmol/L glucose at pH 7.4 with osmolarity adjusted to 310 mmol/kg. Otoliths were gently removed with Dumont tweezers (110 mm, 0.1*0.06 mm tip) and a Tungsten dissecting probe (50 mm, 0.5 mm diameter rod). The tissue was torn into pieces as small as possible under sterile conditions with fine ophthalmic tweezers under an Olympus SZ61 dissecting

microscope using the method described by Neng et al. (Neng et al., 2013b). After the tiny fragments of tissue resettled by gravity, they were repositioned to uniform density with a needle (50 mm, 0.5 mm diameter rod). The tiny fragments were then selectively cultured in one of three specific growth media, each specifically formulated to support the growth of either ECs, PCs, or PVM/Ms.

2.3 EC, PC, and PVM/M growth media

The growth medium for selection of ECs (100 ml) consisted of 20 ml FBS (fetal bovine serum, catalog # F2442, Sigma), 76 mL CS-C (cell systems corporation) medium without serum (catalog # C1556, Sigma), 1 ml of penicillin-streptomycin solution (catalog # P4333, Sigma), 1 ml of Heparin sodium salt 10 mg/mL (catalog # H3393, Sigma), and 2 ml of ECGF (endothelial cell growth factor, catalog # E9640, Sigma). 0.1mmol/L Bromodeoxy Uridine (5-Bromo-2-DeoxyUridine, BrdU) (catalog # B5002, Sigma) was added to the EC growth medium on day 2 to suppress non-specific cell growth. The PC growth medium (100 ml) consisted of 10 ml of FBS (catalog # F2442, Sigma), 1 ml of penicillin-streptomycin solution (catalog # P4333, Sigma), 1 ml of PC Growth Supplement 100 × (catalog # 1252, Science), and 88 ml of DMEM (Dulbecco's modified eagle's medium) low glucose (catalog # 11885-084, Life Technologies). PEDF (pigment epithelium-derived factor, catalog # SRP4988, Sigma) at a concentration of 100 nM was added on day 2 to the PC medium (Yamagishi et al., 2005). The PVM/M growth medium (100 ml) consisted of 10 ml of FBS (catalog # F2442, Sigma), 20 μl gentamicin/amphotericin B solution (catalog # 50-0640, Life Technologies), 0.2 mM$CaCl_2$, 1 ml of HMGS (human melanocyte growth supplement, catalog # S-002-5, Life Technologies), and 88.8 ml of medium 254 CF (calcium-free, catalog # M-254CF-500, Life Technologies).

2.4 Immunohistochemistry and fluorescence microscopy

The mice were deeply sedated with ketamine hydrochloride (100 mg/kg, intramuscularly) and 2% xylazine hydrochloride (10 mg/kg, Abbott Laboratories, USA), and intravascularly perfused through the left ventricle with phosphate-buffered saline (PBS, pH 7.4), followed by fixation with 4% paraformaldehyde (PFA). The vestibular sacculus, utriculus, and ampullae of the semicircular canal tissue were gently isolated, harvested, and fixed in 4% PFA overnight at 4° C, and then rinsed in PBS to remove any residual PFA. Immunohistochemistry was performed as previously described (Zhang et al., 2013). Tissue samples were permeabilized in 0.5% Triton X-100 (Sigma) for 1 h and immunoblocked with a solution of 10% goat serum (alternatively 10% donkey serum) and 1% bovine albumin in 0.02 M PBS for 1 h. For immunofluorescence double labeling, tissues were blocked with 1% fish gelatin solution (G7765 Sigma) for 1 h. The specimens were incubated overnight at 4° C with the primary antibodies (listed in Table 1) diluted in 1% BSA-PBS. After 30 min washes in PBS, the samples were incubated with the secondary antibodies (listed in Table 1) for 1 h at room temperature. Capillaries were labeled with the lectin Griffonia Simplicifolia IB4 (GS-IB4) conjugated to Alexa Fluor 568 (catalog # I21412, Life Technologies). The tissues were washed for 30 min, mounted (H-1000, Vector Laboratories, USA), and visualized under an FV1000 Olympus laser-scanning confocal microscope. Controls were prepared by replacing primary antibodies with overnight incubation in 1% BSA-PBS.

2.5 Staining frozen tissue sections

Cochleae from young mice age 8–12d were isolated and fixed in 4% PFA overnight. After decalcification in bone decalcifier (DCODEQT, Decal Chemical Corporation, USA) overnight, the cochleae were dehydrated with 30% sucrose and embedded with OCT. Seven-micrometer sections of the cochleae were cut in the mid-modiolar plane. The crysolides were washed with PBS for 15 min to remove the OCT component, and sections permeabilized in 0.5% Triton X-100 (Sigma) for 30 min and incubated in 10% normal goat serum (or other similar serum) diluted in PBS for 1 h to block nonspecific binding sites. The sections were incubated for 12 - 16 hrs with a primary antibody (for antibody information, see Table 1) at 4°C. Subsequently, the sections were exposed to an appropriate fluorescence-conjugated secondary antibody (Table 1), and the GS-IB4 conjugated to Alexa Fluor 488, Alexa Fluor 568, or Alexa Fluor 647 at 37°C for 1 h. The tissues were washed for 30 min, mounted (H-1000, Vector Laboratories, USA), sealed in 20% glycerol, and visualized under an FV1000 Olympus laser-scanning confocal microscope. Controls were prepared by replacing primary antibodies with overnight incubation in 1% BSA-PBS.

2.6 Immunolabeling of primary cell lines

The cells at the third passage were fixed in 4% PFA (pH 7.2) for 15 min at room temperature, washed in 2 ml of PBS (three times for 10 min), permeabilized in 0.5% Triton X-100 for 3 min at room temperature, washed in 2 ml of PBS (three times for 10 min), and incubated with a blocking solution at room temperature for 1 h. The cells were then incubated with primary antibodies diluted in a 1% BSA-PBS solution overnight at 4° C, washed in 2 ml of PBS (three times for 10 min), and incubated with secondary antibodies diluted in 1% BSA-PBS solution for 1 h at room temperature. The cells were washed in 2 ml of PBS (three times for 10 min) and imaged under a confocal laser microscope. The antibodies are described in Table 1.

2.7 Visualization of EC, PC, and PVM/M morphology

Cells were double labeled with Alexa Fluor 488-phalloidin diluted in 1% BSA-PBS solution for 1 h at room temperature (for visualization of the cytoskeleton) in addition to labeled for marker proteins. The cells were washed in 2 ml of PBS (three times for 10 min) and imaged under an FV1000 Olympus laser-scanning confocal microscope.

2.8 Reverse transcription-polymerase chain reaction (RT-PCR)

ECs, PCs, and PVM/Ms at the third passage were detached with a solution of trypsin-EDTA, collected in a 5 ml polypropylene round-bottom tube, and centrifuged at 300 g for 5 min. RNA was extracted with an RNeasy micro kit, cDNA synthesized with an RETROscript kit for RT-PCR, both used according to the manufacturer's instructions. The following reaction conditions were used for the RT-PCR: 44° C for 1 h; 92° C for 10 min; then hold at 4° C. Genes of interest included ng2, pdgfrβ, desmin, cd34, glut1, vwf, gstα4, mitf, cd68, and *cd11b*. Forward and reverse primers (see Table 2) and reagents in the RETROscript kit were prepared according to the manufacturer's instructions. PCR products were separated and analyzed by 1.5% agarose gel electrophoresis.

2.9 Cell counts

The cells (first passage, ~7 - 10 d) were detached from the culture dish with a solution of Trypsin-EDTA (catalog # T4049, Sigma) and counted with a hemacytometer (Model no. 1483, Hausser Scientific, Horsham, PA, USA). The mirror-like polished surface was carefully cleaned with ethanol, with a cover slip placed over the counting surface prior to adding the cell suspension. The diluted cell suspension (approximately 10 μl) was introduced into one of the V-shaped wells and allowed to run under the cover slip. Cell counts in 4 large corner squares were recorded, and care was taken to avoid count of obvious cell debris. Cell concentration per ml (and total number of cells) was determined using the following calculation: Cells per ml = the average count per square * the dilution factor * 10^4. The same procedure was done after 7 - 10 d (~ third passage).

2.10 Purity assessment with fluorescence-activated cell sorting (FACS)

ECs, PCs, and PVM/Ms at the third passage were detached with a solution of Trypsin-EDTA (catalog # T4049, Sigma). The cells were gently washed in 2 ml of culture medium and centrifuged at 300g for 5 min at 4° C. The supernatant was carefully aspirated. The cell pellet ($1*10^7$ cells/ml) was re-suspended in its own culture medium and incubated in the dark with different antibodies for 30 min at 4° C. ECs were incubated with CD34 (Table 1) at a concentration of 10 μl/10^6 cells (in 100 μl) for 30 min, washed in culture medium, and incubated with Alexa Fluor 568-conjugated goat anti-rabbit antibody (Table 1) for 20 min. PCs, incubated with phycoerythrin-conjugated rat mAb for PDGFRβ (catalog # ab93534, Abcam) at a concentration of 0.5 μg/ml. Rat IgG phycoerythrin (catalog # ab37368, Abcam), at a concentration of 0.2 μg/ml, served as the isotype control. PVM/Ms were incubated with CD68 (Table 1) at a concentration of 10 μl/10^6 cells (in 100 μl) for 30 min, washed in culture medium, and incubated with Alexa Fluor 488-conjugated goat anti-rat antibody (Table 1) for 20min. The cells were centrifuged at 300 g for 5 min at 4° C and re-suspended in their own culture medium. The cells were analyzed as soon as possible after the final wash using a BD influx cell sorter.

2.11 Transwell monolayer permeability assay

Trans-endothelial permeability of the endothelial cell monolayer to FITC-dextran (MW, 70 kDa) was measured according to the manufacturer's instructions (catalog # ECM 644, vascular permeability assay kit; Millipore, Billerica, MA, USA) and described in our previous study(Neng et al., 2013b) . Briefly, FITC-dextran (diluted at 1 : 40 in serum free medium) permeates through the endothelial cell monolayer into the basolateral chamber. The amount of dextran accumulating in the basolateral chamber is an indicator of permeability. FITC-dextran fluorescence was assessed with a multi-well microplate reader (TECAN GENios ELISA reader, TecanGroup Ltd.) at excitation and emission wavelengths of 485 and 535 nm.

2.12 *In vitro* matrigel angiogenesis Assay

The newly generated primary cell lines were used to investigate the intercellular interactions between ECs and PCs in an angiogenesis model. The two different angiogenesis models developed in this study included culture of (1) ECs only and (2) ECs + PCs in matrigel

matrix. 130 μl ice-cold matrigel basement membrane matrix (catalog # 354234, BD Bioscience, Franklin Lakes, NJ) was added to each well of the LabTek chambered cover glass (catalog # 12565338, Thermo Scientific Nunc, USA) using chilled pipettes and allowed to polymerize for at least 30 min in a 37° C, 5% CO_2 incubator. The BD matrigel basement membrane matrix contains epidermal growth factor, insulin-like growth factor, fibroblast growth factor as well as other growth factors. The three cell types were distinguishably stained with different cell tracker dyes. Cells were harvested by centrifugation, re-suspended in pre-warmed cell-Tracker dye working solution (10 μM dye), and incubated at 37° C for 30 min. The working solution was replaced with culture medium and the cells were incubated for another 30 min at 37° C. After staining, the cells were seeded on the matrigel matrix to initiate proliferation. A 100 μl suspension of ECs ($3.0*10^5$ cells/mL), labeled with a Cell Trace™ Violet Cell Proliferation Kit (catalog # C34557, Life Technologies, USA), was plated on the matrigel matrix for 5 hrs before a 50 μl suspension of PCs ($3.0*10^5$ cells/mL), labeled with CellTracker Red CMTPX (catalog # C34552, Life Technologies, USA), were added to the matrix. The cell model was imaged under a confocal microscope for assessment of tubular network branching at 12 hrs and 24 hrs post seeding.

2.13 Statistics

All statistical analyses were performed using Graph Pad Prism 5.0, with data presented as means ± SEM.

3. Results

3.1 Preparation of the vestibular end-organ explants and selective culture of cells in a specific culture medium

The vestibular end-organs were dissected from the inner ear under sterile conditions from mice aged P8 - P12 and placed in cold artificial perilymph solution (Figure 1A). Vestibular explants, including the sacculus, utriculus, and three ampullae of the semicircular canal, were gently isolated. Cell lines were established from a pool of six end-organs (Figure 1B) torn into tiny fragments under a sterile dissecting microscope. The tissue fragments were uniformly seeded in a collagen I coated tissue culture dish (Figure 1C). In general, multiple cell clusters form around the explanted fragments by day 1 or 2 (Figure D-F) and spread over the entire surface of the dish by day 7 - 10 (Figures J-L).

The fragments of vestibular end-organs are comprised of a mixture of ECs, PCs, PVM/Ms, and other non-blood barrier component cells. To produce each primary cell line, selective growth medium in combination with additional treatments was used. For example, to produce the EC cell line, EC culture medium (see Materials and Methods) was used. In addition, BrdU, a pyrimidine analogue of thymidine, was added to the medium on day 2 and remained in the culture medium for an additional 4 days to maximally inhibit proliferation of non-EC cells such as fibroblasts (Sil et al., 1997). With these medium selective methods, approximately $4 \pm 1.5* 10^4$ ECs were generated by day 7 - 10 in the initial (P1) stage (shown in Figure 1a). ECs were passaged at a split ratio of 1 : 2 and incubated in EC growth medium at 37° C and 5% CO_2. Cell growth was checked every 2 d under a phase-contrast microscope and the medium changed every 2 d for about 5 - 7 d (second passage, P2).

Passage three was also done at a split ratio of 1 : 2 and the cells grown an additional 5 - 7 d. Approximately $1.5 \pm 0.5*10^6$ ECs were obtained in the third passage.

PCs were produced with PC culture medium with the addition of PEDF added to the culture medium on day 2 at a concentration of 100 nM. In our experiment, we found that clusters of PCs around the tissue fragments began to form by day 2 (shown in Figure 1 E). Individual cells were seen to spread rapidly by day 4 as shown in Figure 1H. The proliferation was quite marked by day 7 with the formation of large colonies (Figure 1K). About $4 \pm 1*10^4$ PCs were harvested by day 7 - 10 in the initial (P1) stage (Figure 1b). Passage of the PCs in the growth medium gave approximately $10 \pm 1*10^5$ PCs in the third passage.

PMM/Ms, a hybrid cell with characteristics of both macrophage and melanocyte, were produced in PVM/M culture medium containing HMGS (human melanocyte growth supplement). Approximately $10 \pm 1*10^4$ PVM/Ms were generated by day 7-10 in the initial (P1) stage, as shown in Figure 1c. The cells were then passaged and further grown in the specific PVM/M growth medium. The third passage yielded about $9 \pm 1*10^5$ PVM/Ms.

3.2 Pre-validation of barrier component cell marker proteins *in situ* in surface prepared whole mounted vestibular end-organs

In this study, at least two marker proteins were used to identify each primary cell phenotype. The markers were pre-verified *in situ* in whole mounted tissue preparations (Figures 2A, 2F and 2K). ECs are known to have different protein expression in different tissues. Endothelial cells express a variety of marker proteins in different tissues, including Von Willebrand factor (vWf), VE-cadherin (CD44), platelet/EC adhesion molecule-1 (PECAM-1, CD31), vascular endothelial growth factor receptors (VEGFRs), CD34, and glucose transporter 1 (Glut1)(Navone et al., 2013; Pusztaszeri et al., 2006). Despite the variety of protein expression, Von Willebrand factor is considered the gold standard for EC identification (Middleton et al., 2005). Expression of vWF in endothelial cells in human vestibular capillaries was previously reported by Masuda M et al. (Masuda et al., 1997). In the present study, we identified ECs from the vestibular system in confocal microscope images on the basis of vWF expression. As a further confirmation, endothelial cell lines were assessed for expression of the marker protein Glut1. We also stained vessels with fluorescent conjugated GS-IB4 for visualization (Zhang et al., 2013). We found the two EC markers prominently expressed in the capillaries of all three vestibular end-organs (Figures 2B-E).

PCs are smooth muscle like cells which, in different tissues, are heterogeneous in morphology and expression of marker proteins (Shi et al., 2008). PCs were initially recognized on the basis of their distinctive shape and location, but are now most commonly identified with molecular markers such as α-smooth muscle actin (α-SMA), tropomyosin, desmin, nestin, and PDGFRβ. PCs are not characterized by specific marker proteins. Rather the expression varies with the type of vessel. Thus PCs are best identified on the basis of multiple markers and morphological features (Armulik et al., 2005). In this study, we identified PCs on the basis of PDGFR-β and desmin expression. Cochlear PCs express two marker proteins, desmin and NG2, which are not found in ECs and PVM/Ms of whole mounted stria vascularis tissue (Neng et al., 2013b). In this study, we confirmed the

vestibular PCs also express PDGFR-β and desmin by immunolabeling whole mounted tissue of the sacule and utricle with antibodies for the proteins (shown in Figures 2G-J).

PVM/Ms in the stria vascularis are a hybrid cell type not fitting the phenotype of the classical macrophage (Neng et al., 2013b; Zhang et al., 2012). PVM/Ms display characteristics of macrophage and melanocyte, and, correspondingly, express both macrophageand melanocyte marker proteins (Neng et al., 2013b; Shi, 2010; Zhang et al., 2012). Like PVM/Ms in the stria vascularis, whole mounted PVM/Ms in the vestibular system express both protein phenotypes (Zhang et al., 2013). In this study, PVM/M primary cultured cells were shown to express multiple cell marker protein genes, including GSTα4 (a melanocyte marker protein) and CD68 (a macrophage marker protein)(shown in Figures L-O).

We have also double immunolabeled each cell phenotype *in vivo* for co-expression of two marker proteins and confirmed the three cell line marker proteins used for identifying the primary cell phenotypes are naturally expressed in the vestibular end-organs (as shown in Fig.2Q-S). Furthermore, we pre-validated barrier component cell marker proteins *in vivo* in frozen tissue section preparations. The frozen tissue section preparation gives an overview of cell type distribution in different regions of the vascular apparatus [see attached Supplemental Figures 1(a), (b), and (c)].

3.3 Validation the PCs and PVM/Ms are not neurons of the vestibular end-organs *in situ*

The end organs are a mixture of cell types, including a large number of neurons which may express the same marker proteins as PCs and PVM/Ms express. Since this would present a problem for validating cell purity, we investigated whether any PC or PVM/M markers are also expressed by neurons. We triply labelled tissues with antibodies for a PC marker, the neuron marker NF-160, a marker widely used for neuron identification (Yang et al., 2000), and GS-IB4, a marker for capillaries. We found that the fluorescence signal for the PC marker protein desmin (red, arrow, panel A of Figure 3) does not overlap the fluorescence signal for NF-160 (green, arrow). Neither does the PVM/M marker protein, CD68 signal (red, arrow), overlap the signal for NF-160 (green, panel B of Figure 3). Our results confirm that neurons do not express desmin or CD68. Our result showed that some of the NF-160 positive cells were co-labeled with COX10, a Schwann cell marker protein (shown in panel C and D of Figure 3). We also found that those cells were not closely associated with vessels labeled with GS-IB4 (blue). Our results demonstrate the validity of using the neuron markers SOX10 and NF-160 for confirming the purity of vestibular cell lines *in vitro*. We also demonstrated that the PC marker desmin and PVM/M marker CD68 used for cell line identification were not expressed in neurons.

3.4 Validation of the cell line phenotype *in vitro*

The phenotype of PCs, PVM/Ms, and ECs was validated by immunostaining for marker proteins and verifying gene expression with RT-PCR. Figures 4A-C are DIC images of cultured ECs, PCs, and PVM/Ms at the third passage. Figures 4D-I show the three cell lines immune-stained with antibodies for their respective marker proteins. Figures 4J-L show the corresponding RT-PCR gene analysis for each cell line. Genes for *vWF, cd34,* and *glut1*

were detected in the EC cell line. Genes of *pdgfrβ, desmi*n, and *ng2* were detected in the PCs. Two melanocyte marker genes, *mitf* and *gsta4*, and two macrophage marker genes, *cd68* and *cd11b*, were detected in the PVM/M cell line.

3.5 Validation of the cell lines by morphology

The phenotype of the ECs, PCs, and PVM/Ms was also validated by morphological analysis. Cells were stained with phalloidin and a specific cell marker for visualization. Figures 5A-C are DIC images of cultured ECs, PCs, and PVM/Ms at the third passage. ECs have a flat, elongated, and generally cuboidal morphology, consistent with an earlier report (Gerrity et al., 1977) (Figure 5D). The PVM/Ms, previously identified as melanocytes (Zhang et al., 2012), exhibit unique dendritic processes (Figure 5E). The cultured PCs display as large, flat, and stellate shaped cells with a broad filopodial morphology (Figure 5F). Figures 5G-I demonstrate the characteristics of each cell type under high magnification.

3.6 Validation the PC and PVM/M cell lines are not neurons in the vestibular end-organs *in vitro*

Although we validated the PC and PVM/M cell line with immune-typing and gene analysis, we also further explicitly tested for the level of neuron contamination. We double labeled cell lines with either PC or PVM/M marker proteins and neuron or Schwann cell markers. The latter included NF-160 and SOX10, both widely used as markers for neurons and Schwann cells (Brehmer et al., 2002; Crisan et al., 2008; Nonaka et al., 2008; Yang et al., 2000). We also examined neuron genes (NF-160), along with PC or PVM/M marker genes, to further confirm the PC or PVM/M phenotype. Figure 6 shows that neither the PC marker PDGFRβ nor the PVM/M marker CD68 co-labelled with NF-160 or SOX10. Multiple gene analysis showed the PC cell line to express PC marker genes including desmin, PDGFRβ, and NG2, but not the neuron gene NF-160.

3.7 Assessment of cell purity

Cell purity was assessed and validated by FACS. Figures 7A-C show DIC images of trypsin-treated detached cells at passage three before FACS analysis. Figures 7D-F show confocal images of the detached cells with single marker labeling. The merged images in Figures 7G-I show the considerable overlap between marker protein labeled cells and the cells viewed under bright field.

The purity of each cell line, validated by FACS, is shown in bivariate histograms (Figures 7J-L). The mean purity from multiple FACS analyses is ECs 94 ± 5 % (mean ± SEM, $n = 3$), PCs 92 ± 2% (mean ± SEM, $n = 5$), and PVM/Ms 93 ± 2 % (mean ± SEM, $n = 3$).

3.8 Utility of generated cell lines and validation of functional ECs and PCs

The primary cell lines enable direct study of intercellular interaction between ECs, PCs, and PVM/Ms in mono- and co-culture. In particular, BLB permeability of the EC-monolayer can be studied *in vitro*. The EC monolayer is shown in Figure 8, with its expression of tight junction proteins and characteristic “physical barrier.” Figures 8A-E respectively show cell-cell TJ protein expression of cytosolic zonula occludens-1 (ZO-1), occludin, VE-cadherin, and JAM1 at the transcript and protein levels. Permeability is assessed in the established

endothelial monolayer by measuring the flux of 70 kDa fluorescent dextran across the EC-monolayer (shown in Figure 8F). The degree of EC-monolayer leakage is determined from the intensity of FITC-dextran fluorescence in the basolateral chamber. For example, low and stable endothelial monolayer permeability to FITC-dextran was found at day 7 following seeding with 200 μl vestibular ECs at a concentration of 3.4×10^5 cells/ml on the transwell insert (Figure 8F).

The primary cell lines also enable investigation of angiogenesis. For example, the effect of interaction between ECs and PCs on the growth of endothelial tubules can be studied as demonstrated in Figures 8G-J. We found a dramatically different pattern of branch formation between models of ECs alone and ECs co-cultured with PCs. The examples in Figure 8G demonstrate the effect of intercellular interaction on tubule formation in EC alone and EC/PC co-culture models at 12 hours and 24 hours after cell seeding in a 3D matrigel assay. We noticed a more robust sprouting angiogenesis in the presence of PCs. The cell culture–based *in vitro* models offer a unique opportunity to study cell-cell interactions and role of individual cell barrier component cells in BLB function.

4. Discussion

The blood-labyrinth barrier (BLB) in the inner ear is a highly specialized capillary network that controls exchanges between blood and shields the inner ear from blood-born toxic substances and selectively passes ions, fluids, and nutrients to the ear, playing an essential role in the maintenance of inner ear homeostasis.

Blood-tissue barriers in the different regions of the inner ear make up the inner ear BLB system as a whole, including major blood-tissue barriers in the cochlear lateral wall and the blood-tissue barrier in the vestibular system. The physical blood-tissue barrier is comprised of ECs in the strial microvasculature, elaborated tight and adherens junctions, and accessory cells such as PCs, basement membrane (BM), and PVM/Ms, which together form a complex blood-tissue barrier with region-specific features(Shi, 2016).

Previously, using a similar growth medium–based approach, we obtained cochlear ECs, PCs, and PVM/Ms from the blood-tissue barrier in the stria vascularis of young mice (Neng et al., 2013a; Neng et al., 2013b). These cell line models, in combination with different *in vitro* co- and triple-culture models, enable us to study the physical interactions between ECs, PCs, and PVM/Ms as well as to begin to understand the signaling between cells which regulates vascular permeability and provides a proper environment for hearing function in the cochlea (Neng et al., 2013a).

Similar to the structure of the blood-tissue barrier in the stria vascularis, the blood-tissue barrier in the vestibular system is comprised of small volume end-organs with high anatomical complexity. Isolating PCs, ECs, and PVM/Ms from such small end-organ tissues is a substantial challenge. In this study, we have adapted the method for obtaining cell lines from the stria vascularis to the vestibular system, and we demonstrated the three cell lines can also be successfully established from vestibular tissue. Specifically, we collected utrical, sacule, and ampullar samples from young (P8-12 day old) mouse ear and manually minced

them into “tiny” fragments. The cochlear cells in mice at this age are still highly proliferative. The “tiny” fragments of the “vestibular end-organ unit” are small enough to allow barrier component cells access to the culture medium. In this method, each barrier cell phenotype is selected and nurtured by choice of culture medium. Overall, the method produces an expanded and homogenous population of primary culture cells from the vestibular system.

Most established methods for isolating blood/tissue barrier cells, including ECs and PCs, were developed on large tissue masses, such as brain, retina, skeletal muscle, skin, and fetal tissues (Abbott et al., 2012; Bryan et al., 2008; Katyshev et al., 2012; Maier et al., 2010; Mogensen et al., 2011; Nees et al., 2012; Siow, 2012). These methods are typically complex procedures, involving multiple steps of enzymatic digestion and gradient density centrifugation. The stringency of the procedure is also reported to cause some level of damage to barrier cells such as ECs (Bernas et al., 2010). Our method, however, differs from previously published methods. This method does not require chemical digestion with collagenase. Sequential sieving steps are not required for separating large tissue fragments from single cells, nor are extra efforts required to collect appropriately sized fragments from the digested suspension. Primary cell types are generated from culturing in specialized media. For example, EC proliferation is specifically promoted by adding an endothelial growth factor to the culture medium. In contrast, non-specific EC growth can be inhibited by adding a synthetic nucleoside, BrdU, to the EC culture medium, as reported by Sil (Sil et al., 1997). On the other hand, PCs and PVM/Ms are produced by adding the growth factors PEDF or melanocyte growth factor to the medium. PEDF growth factor is essential for promoting vestibular PC growth (Neng et al., 2013b), similar to what we found in PC cell lines developed from stria vascularis tissue (Neng et al., 2013a). Also consistent with PVM/Ms in the stria vascularis, melanocyte growth factor potently and selectively stimulates PVM/M proliferation and growth.

In this study, each cell line (PC, PVM/M, and EC) was validated by immune-phenotyping for expression of cell marker proteins, profiling the gene-expression, and ascertaining the morphological characteristics. For example, PCs are smooth muscle like cells, which, in different tissues, are heterogeneous in morphology and express different marker proteins (Nehls et al., 1991). Generally they cannot be identified by a single marker protein. Instead, PCs are often identified on the basis of a set of marker proteins in combination with their morphological features as described by others (Armulik et al., 2005). In this study, we identified the PCs on the basis of the expressions of PDGFRβ and desmin marker proteins, which are also used to characterize PCs in the stria vascularis (Shi et al., 2008). The end organs are known to contain a mixture of many unwanted cell types such as Schwann cells and neurons (Skaper et al., 1980). To determine whether the generated PC cell line was contaminated by Schwann cells and neurons, we examined the cell line with a specific antibody for SOX 10, a marker protein for Schwann cells (Finzsch et al., 2010; Nonaka et al., 2008), and a specific antibody for NF-160, a marker protein for neurons(Yang et al., 2000). Our data shows that no detectable signals for both SOX10 and NF-160 in the generated primary PC cell line.

Similar to PCs, ECs are heterogeneous in protein expression from tissue to tissue. ECs express a variety of marker proteins, including vWF, VE-cadherin (CD44), platelet/EC adhesion molecule-1 (PECAM-1, CD31), vascular endothelial growth factor receptors (VEGFRs), CD34, and Glut1 (Navone et al., 2013; Pusztaszeri et al., 2006). A comparative study by Middleton et al. (Middleton et al., 2005) found that vWFis the gold standard for EC identification in human tissue. vWF expression in vestibular capillary ECs, previously reported by Masuda et al. (Masuda et al., 1997), was pre-validated in our immunofluorescence labeling. In our study, we validated the EC cell line from vestibular tissue based on expression of vWF and Glut1, the latter a second well-known EC marker protein, as well as on the basis of features such as a flat and generally cuboidal morphology, as shown in Figure 5.

PVM/Ms in the stria vascularis are a hybrid cell type that does not fit the phenotype of the classical macrophage (Neng et al., 2013b; Zhang et al., 2012). The PVM/Ms display characteristics of macrophage and melanocyte, expressing both macrophage marker proteins and melanocyte proteins (Neng et al., 2013b; Zhang et al., 2012). Like PVM/Ms in whole mounted stria vascularis tissue, PVM/Ms in the vestibular system express both protein phenotypes (Zhang et al., 2013). In this study, PVM/M primary culture cells were shown to express multiple cell marker proteins, including GSTα4 (melanocyte marker protein), Mitf (melanocyte marker protein), CD68 (macrophage marker protein), and CD11b (macrophage marker protein). Genes related to the proteins, including for expression of CD68 and GSTα4, were found in the PVM/Ms both *in vivo* and *in vitr*o. The PVM/Ms were negative for NF-160, a marker protein often expressed in neurons (Ray et al., 1993; Raymond, 1987).

The method of producing cell lines from vestibular tissue is technically practicable, requires no enzymatic treatment, and yields consistent results. However, when comparing the method in strialand vestibular tissue, the yield of primary cell lines generated from vestibular tissueis lower than from strial tissue. For example, approximately 1 - $2*10^6$ (ECs), 9 - $11*10^5$ (PCs), and 8 - $10*10^5$ (PVM/Ms) at P3 are obtained from the vestibular end-organs of six mice, compared to 2 - $3*10^6$ (ECs), 1 - $2*10^6$ (PCs), and 1.5 - 2.5* 10^6 (PVM/Ms) generated from the BLB of the stria vascularis (Neng et al., 2013b). Nonetheless, the cell numbers obtained from the vestibular tissue of six mice is still sufficient for establishing an *in vitro* co-culture system.

The individual roles of blood barrier component cells have rarely been investigated. The newly generated primary cell lines can be used in cell culture-based *in vitro* models, offering a unique opportunity to directly study the intercellular interactions between ECs, PVM/Ms, and PCs, the specific role of each phenotype on BLB permeability and angiogenesis, and tissue-specific characteristics of the cochlear blood/tissue barrier. For example, the cell lines established by this method will enable us to directly study how BLB integrity is controlled and how barrier integrity (e.g., vascular permeability) is influenced by different pathogens, such as viral infection, long thought to cause hydrops in the inner ear and Ménière's disease. EC-monolayer leakage, reflecting vascular permeability, can be determined in an EC-monolayer by measuring the degree of extravasated FITC-dextran from the EC monolayer under physiological and pathological conditions. The mechanism related to the change in monolayer permeability can also be investigated by measuring the level of tight junction

protein expression, including occludin, claudins, ZO-1, and the junctional adhesion molecules (JAMs, Jam1, 2, 3), in the EC monolayer, as shown in Figure 8A. The newly generated primary cell line from the vestibular system will also allow us to study how cell-cell interactions affect vascular stability. For example, the role of PCs on EC proliferation and angiogenesis can be determined using a 3D matrigel matrix co-culture model, as shown in Figure 8C.

The blood barrier integrity when it is normally functioning plays an essential role in maintaining ion and fluid homeostasis (flow volume, pressure, ion concentration, and osmolarity). Disruption of the BLB has been associated with hearing and balance dysfunction, including autoimmune inner ear disease, Ménière's disease, and meningitis-associated labyrinthitis. As we gain better understanding of the control mechanisms in the blood barrier, particularly those responsible for its integrity, we may be able to improve treatments for patients who experience vestibular dysfunction due to vascular disruption.

Supplementary Material

Refer to Web version on PubMed Central for supplementary material.

Acknowledgments

This work was supported by National Institutes of Health grants NIH NIDCD DC008888S1 (XS), NIH NIDCD R01 DC010844 (XS), R21 DC1239801 (XS), and NIH P30-DC005983 (Peter Barr-Gillespie).

Abbreviations

BBB	blood-brain-barrier
BLB	blood-labyrinth barrier
BRB	blood-retina-barrier
BrdU	Bromo-2-DeoxyUridine
CF	calcium-free
CS-C	cell systems corporation
DMEM	Dulbecco's modified eagle's medium
EC	endothelial cell
ECGF	endothelial cell growth factor
FACS	fluorescence-activated cell sorting
FBS	fetal bovine serum
FITC-dextran	fluorescein isothiocyanate dextran
Glut1	glucose transporter 1
GS-IB4	lectin Griffonia Simplicifolia IB4

HMGS	human melanocyte growth supplement
JAM1	junctional adhesion molecule 1
Mitf	microphthalmia-associated transcription factor
PC	pericyte
PDGFRβ	platelet-derived growth factor receptor, beta
PEDF	pigment epithelium-derived factor
PVM/Ms	perivascular-resident macrophage-like melanocytes
TJ	tight junction
vWF	Von Willebrand factor

References

Abbott NJ, Dolman DE, Drndarski S, Fredriksson SM. An improved in vitro blood-brain barrier model: rat brain endothelial cells co-cultured with astrocytes. Methods Mol Biol. 2012; 814:415–30. [PubMed: 22144323]

Armulik A, Abramsson A, Betsholtz C. Endothelial/pericyte interactions. Circulation research. 2005; 97:512–23. [PubMed: 16166562]

Ballarin C, Peruffo A. Primary cultures of astrocytes from fetal bovine brain. Methods Mol Biol. 2012; 814:117–26. [PubMed: 22144304]

Bernas MJ, Cardoso FL, Daley SK, Weinand ME, Campos AR, Ferreira AJ, Hoying JB, Witte MH, Brites D, Persidsky Y, Ramirez SH, Brito MA. Establishment of primary cultures of human brain microvascular endothelial cells to provide an in vitro cellular model of the blood-brain barrier. Nat Protoc. 2010; 5:1265–72. [PubMed: 20595955]

Bowman PD, Ennis SR, Rarey KE, Betz AL, Goldstein GW. Brain microvessel endothelial cells in tissue culture: a model for study of blood-brain barrier permeability. Ann Neurol. 1983; 14:396–402. [PubMed: 6638956]

Bowman PD, Betz AL, Ar D, Wolinsky JS, Penney JB, Shivers RR, Goldstein GW. Primary culture of capillary endothelium from rat brain. In Vitro. 1981; 17:353–62. [PubMed: 6263791]

Brehmer A, Schrodl F, Neuhuber W. Morphological phenotyping of enteric neurons using neurofilament immunohistochemistry renders chemical phenotyping more precise in porcine ileum. Histochemistry and cell biology. 2002; 117:257–63. [PubMed: 11914923]

Bryan BA, D'Amore PA. Pericyte isolation and use in endothelial/pericyte coculture models. Methods Enzymol. 2008; 443:315–31. [PubMed: 18772023]

Crisan M, Huard J, Zheng B, Sun B, Yap S, Logar A, Giacobino JP, Casteilla L, Peault B. Purification and culture of human blood vessel-associated progenitor cells. Curr Protoc Stem Cell Biol. 2008 Chapter 2, Unit 2B 2 1-2B 2 13.

Cucullo L, McAllister MS, Kight K, Krizanac-Bengez L, Marroni M, Mayberg MR, Stanness KA, Janigro D. A new dynamic in vitro model for the multidimensional study of astrocyte-endothelial cell interactions at the blood-brain barrier. Brain Res. 2002; 951:243–54. [PubMed: 12270503]

Duport S, Robert F, Muller D, Grau G, Parisi L, Stoppini L. An in vitro blood-brain barrier model: cocultures between endothelial cells and organotypic brain slice cultures. Proc Natl Acad Sci U S A. 1998; 95:1840–5. [PubMed: 9465104]

Finzsch M, Schreiner S, Kichko T, Reeh P, Tamm ER, Bosl MR, Meijer D, Wegner M. Sox10 is required for Schwann cell identity and progression beyond the immature Schwann cell stage. J Cell Biol. 2010; 189:701–12. [PubMed: 20457761]

Garlanda C, Dejana E. Heterogeneity of endothelial cells. Specific markers. Arterioscler Thromb Vasc Biol. 1997; 17:1193–202. [PubMed: 9261246]

Gerrity RG, Richardson M, Somer JB, Bell FP, Schwartz CJ. Endothelial cell morphology in areas of in vivo Evans blue uptake in the aorta of young pigs. II. Ultrastructure of the intima in areas of differing permeability to proteins. Am J Pathol. 1977; 89:313–34. [PubMed: 920777]

Invernici G, Ponti D, Corsini E, Cristini S, Frigerio S, Colombo A, Parati E, Alessandri G. Human microvascular endothelial cells from different fetal organs demonstrate organ-specific CAM expression. Exp Cell Res. 2005; 308:273–82. [PubMed: 15936757]

Juhn SK, Hunter BA, Odland RM. Blood-labyrinth barrier and fluid dynamics of the inner ear. Int Tinnitus J. 2001; 7:72–83. [PubMed: 14689642]

Katyshev V, Dore-Duffy P. Pericyte coculture models to study astrocyte, pericyte, and endothelial cell interactions. Methods Mol Biol. 2012; 814:467–81. [PubMed: 22144326]

Lai CH, Kuo KH. The critical component to establish in vitro BBB model: Pericyte. Brain Res Brain Res Rev. 2005; 50:258–65. [PubMed: 16199092]

Laurell GF, Teixeira M, Duan M, Sterkers O, Ferrary E. Intact blood-perilymph barrier in the rat after impulse noise trauma. Acta Otolaryngol. 2008; 128:608–12. [PubMed: 18568492]

Leppens G, Gardner DK, Sakkas D. Co-culture of 1-cell outbred mouse embryos on bovine kidney epithelial cells: effect on development, glycolytic activity, inner cell mass:trophectoderm ratios and viability. Hum Reprod. 1996; 11:598–603. [PubMed: 8671275]

Maier CL, Shepherd BR, Yi T, Pober JS. Explant outgrowth, propagation and characterization of human pericytes. Microcirculation. 2010; 17:367–80. [PubMed: 20618694]

Masuda M, Yamazaki K, Kanzaki J, Hosoda Y. Immunohistochemical and ultrastructural investigation of the human vestibular dark cell area: roles of subepithelial capillaries and T lymphocyte-melanophage interaction in an immune surveillance system. The Anatomical record. 1997; 249:153–62. [PubMed: 9335460]

Middleton J, Americh L, Gayon R, Julien D, Mansat M, Mansat P, Anract P, Cantagrel A, Cattan P, Reimund JM, Aguilar L, Amalric F, Girard JP. A comparative study of endothelial cell markers expressed in chronically inflamed human tissues: MECA-79, Duffy antigen receptor for chemokines, von Willebrand factor, CD31, CD34, CD105 and CD146. The Journal of pathology. 2005; 206:260–8. [PubMed: 15887283]

Mischeck U, Meyer J, Galla HJ. Characterization of gamma-glutamyl transpeptidase activity of cultured endothelial cells from porcine brain capillaries. Cell Tissue Res. 1989; 256:221–6. [PubMed: 2565771]

Mogensen C, Bergner B, Wallner S, Ritter A, d'Avis S, Ninichuk V, Kameritsch P, Gloe T, Nagel W, Pohl U. Isolation and functional characterization of pericytes derived from hamster skeletal muscle. Acta Physiol (Oxf). 2011; 201:413–26. [PubMed: 20969729]

Navone SE, Marfia G, Nava S, Invernici G, Cristini S, Balbi S, Sangiorgi S, Ciusani E, Bosutti A, Alessandri G, Slevin M, Parati EA. Human and mouse brain-derived endothelial cells require high levels of growth factors medium for their isolation, in vitro maintenance and survival. Vasc Cell. 2013; 5:10. [PubMed: 23672996]

Nees S, Weiss DR, Senftl A, Knott M, Forch S, Schnurr M, Weyrich P, Juchem G. Isolation, bulk cultivation, and characterization of coronary microvascular pericytes: the second most frequent myocardial cell type in vitro. Am J Physiol Heart Circ Physiol. 2012; 302:H69–84. [PubMed: 22037185]

Nehls V, Drenckhahn D. Heterogeneity of microvascular pericytes for smooth muscle type alpha-actin. J Cell Biol. 1991; 113:147–54. [PubMed: 2007619]

Neng L, Zhang F, Kachelmeier A, Shi X. Endothelial cell, pericyte, and perivascular resident macrophage-type melanocyte interactions regulate cochlear intrastrial fluid-blood barrier permeability. Journal of the Association for Research in Otolaryngology : JARO. 2013a; 14:175–85. [PubMed: 23247886]

Neng L, Zhang W, Hassan A, Zemla M, Kachelmeier A, Fridberger A, Auer M, Shi X. Isolation and culture of endothelial cells, pericytes and perivascular resident macrophage-like melanocytes from the young mouse ear. Nat Protoc. 2013b; 8:709–20. [PubMed: 23493068]

Nonaka D, Chiriboga L, Rubin BP. Sox10: a pan-schwannian and melanocytic marker. Am J Surg Pathol. 2008; 32:1291–8. [PubMed: 18636017]

Ohtsuki S, Yamaguchi H, Asashima T, Terasaki T. Establishing a method to isolate rat brain capillary endothelial cells by magnetic cell sorting and dominant mRNA expression of multidrug resistance-associated protein 1 and 4 in highly purified rat brain capillary endothelial cells. Pharmaceutical research. 2007; 24:688–94. [PubMed: 17318419]

Pusztaszeri MP, Seelentag W, Bosman FT. Immunohistochemical expression of endothelial markers CD31, CD34, von Willebrand factor, and Fli-1 in normal human tissues. J Histochem Cytochem. 2006; 54:385–95. [PubMed: 16234507]

Ray J, Peterson DA, Schinstine M, Gage FH. Proliferation, differentiation, and long-term culture of primary hippocampal neurons. Proc Natl Acad Sci U S A. 1993; 90:3602–6. [PubMed: 8475109]

Raymond J. In vitro differentiation of mouse embryo statoacoustic ganglion and sensory epithelium. Hear Res. 1987; 28:45–56. [PubMed: 3610860]

Ryan US. Isolation and culture of pulmonary endothelial cells. Environ Health Perspect. 1984; 56:103–14. [PubMed: 6090112]

Rybak LP. Metabolic disorders of the vestibular system. Otolaryngol Head Neck Surg. 1995; 112:128–32. [PubMed: 7816447]

Sakagami M, Sano M, Harada T, Kubo T, Matsunaga T, Sakai S. Morphological study of blood-labyrinth barrier in the vestibular organs under normal and experimental acute hypertensive and acute hypotensive conditions. Acta Otolaryngol. 1986; 101:165–71. [PubMed: 3705947]

Shi X. Resident macrophages in the cochlear blood-labyrinth barrier and their renewal via migration of bone-marrow-derived cells. Cell and tissue research. 2010; 342:21–30. [PubMed: 20838812]

Shi X. Pathophysiology of the cochlear intrastrial fluid-blood barrier (review). Hearing research. 2016; 338:52–63. [PubMed: 26802581]

Shi X, Han W, Yamamoto H, Tang W, Lin X, Xiu R, Trune DR, Nuttall AL. The cochlear pericytes. Microcirculation. 2008; 15:515–29. [PubMed: 19086261]

Sil P, Sen S. Angiotensin II and myocyte growth: role of fibroblasts. Hypertension. 1997; 30:209–16. [PubMed: 9260982]

Siow RC. Culture of human endothelial cells from umbilical veins. Methods Mol Biol. 2012; 806:265–74. [PubMed: 22057458]

Skaper SD, Manthorpe M, Adler R, Varon S. Survival, proliferation and morphological specialization of mouse Schwann cells in a serum-free, fully defined medium. J Neurocytol. 1980; 9:683–97. [PubMed: 7441307]

Stins MF, Gilles F, Kim KS. Selective expression of adhesion molecules on human brain microvascular endothelial cells. Journal of neuroimmunology. 1997; 76:81–90. [PubMed: 9184636]

Sundberg K, Dreij K, Seidel A, Jernstrom B. Glutathione conjugation and DNA adduct formation of dibenzo[a,l]pyrene and benzo[a]pyrene diol epoxides in V79 cells stably expressing different human glutathione transferases. Chem Res Toxicol. 2002; 15:170–9. [PubMed: 11849043]

Tagaya M, Yamazaki M, Teranishi M, Naganawa S, Yoshida T, Otake H, Nakata S, Sone M, Nakashima T. Endolymphatic hydrops and blood-labyrinth barrier in Meniere's disease. Acta Otolaryngol. 2011; 131:474–9. [PubMed: 21198346]

Trune DR. Cochlear immunoglobulin in the C3H/lpr mouse model for autoimmune hearing loss. Otolaryngol Head Neck Surg. 1997; 117:504–8. [PubMed: 9374175]

Xie S, Yang X, Qian G, Wang G. [Culture and characterization of rat lung microvascular endothelial cells]. Zhongguo Ying Yong Sheng Li Xue Za Zhi. 1997; 13:189–90. [PubMed: 10074255]

Yamagishi S, Nakamura K, Takenaka K, Matsui T, Jinnouchi Y, Imaizumi T. Pigment epithelium-derived factor (PEDF) promotes growth of pericytes through autocrine production of platelet-derived growth factor-B. Microvasc Res. 2005; 69:128–34. [PubMed: 15896354]

Yang H, Mujtaba T, Venkatraman G, Wu YY, Rao MS, Luskin MB. Region-specific differentiation of neural tube-derived neuronal restricted progenitor cells after heterotopic transplantation. Proceedings of the National Academy of Sciences of the United States of America. 2000; 97:13366–71. [PubMed: 11087876]

Zhang F, Zhang J, Neng L, Shi X. Characterization and inflammatory response of perivascular-resident macrophage-like melanocytes in the vestibular system. Journal of the Association for Research in Otolaryngology : JARO. 2013; 14:635–43. [PubMed: 23821347]

Zhang W, Dai M, Fridberger A, Hassan A, Degagne J, Neng L, Zhang F, He W, Ren T, Trune D, Auer M, Shi X. Perivascular-resident macrophage-like melanocytes in the inner ear are essential for the integrity of the intrastrial fluid-blood barrier. Proceedings of the National Academy of Sciences of the United States of America. 2012; 109:10388–93. [PubMed: 22689949]

Highlights

- Culture media-based method for establishing primary cell lines from blood barrier cells
- Primary blood barrier component cells with a purity > 90% are obtained in 3 weeks
- The protocol is simple and provides consistent results
- Highly purified primary cell lines enable *in vitro* study of the barrier control function

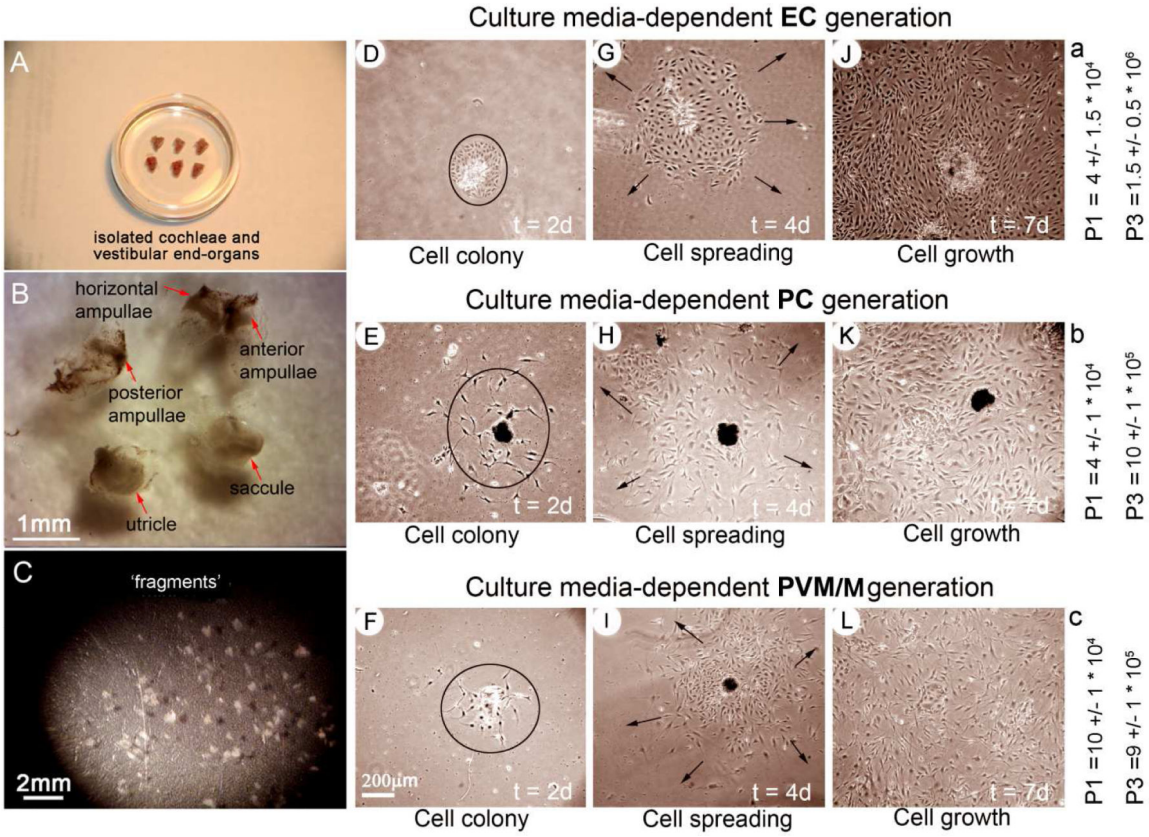

Figure 1.

Outline of steps in expanding primary cells in vestibular end-organ explants. (A) Six ears are needed to produce sufficient cells for each cell line. (B) The vestibular sacculus, utriculus, and ampullae of the semicircular canal tissue are gently dissected under sterile conditions and placed in cold artificial perilymph solution. Vestibular end-organs are 'banked' in fresh culture media under an inverted microscope. (C) The fragments are plated to uniform density in 35-mm collagen I-coated dishes under an inverted microscope. Growth media provide optimal conditions for selective growth of cochlear ECs, PCs, or PVMs. (D-F) Cell clusters (black circles) form around the explanted vestibular end-organ chips by day 2. (G-I) Expansion of the EC, PC, and PVM/M clusters is shown (black arrows). (J-L) Individual ECs, PCs and PVM/Ms spread over the surface of the petri dish by day 7. Generally, all three cell types grow at much same rate. (a-c) Expected population numbers for each cell line at the first and third passage.

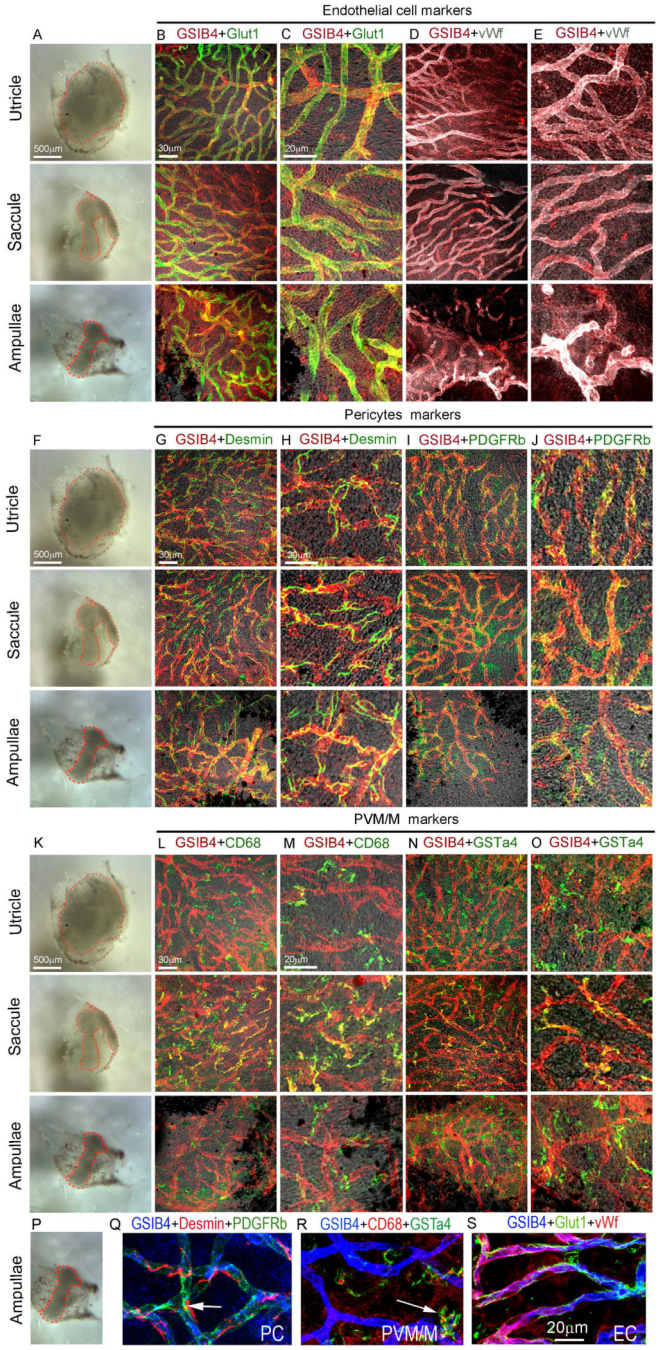

Figure 2.

Immunophenotyping of the barrier cells *in vivo* with a surface preparation of whole mounted vestibular end-organs.(A), (F) and (K) show examples of immuno-phenotyped vestibular end-organs. (B-E) tissues were double labeled with antibodies for the EC marker proteins Glut1 (green) and vWF (gray), while capillaries were labeled by GS-IB4 (red)and viewed under low and high magnification. EC markers are prominently expressed in the capillaries of all three types of vestibular end-organs. (G-J) tissues were double labeled with antibodies for the PC marker proteins desmin (green) and PDGFRβ (green), capillaries by GS-IB4

(red), and the cells viewed under low and high magnification. Vestibular PCs express both PDGFRβ and desmin in immunolabeled whole mounted vestibular end-organs. (L-O) tissues were double labeled with antibodies for the PVM/M marker proteins CD68 (green) and GSTα4 (green), capillaries by GS-IB4 (red), and the cells viewed under low and high magnification. PVM/Ms *in vivo* are shown to exclusively express GSTα4 (melanocyte marker protein) and CD68 (macrophage marker protein). (Q-S) representative confocal projection images show co-expression of two marker proteins respectively in PCs, ECs and PVM/Ms*in vivo*.

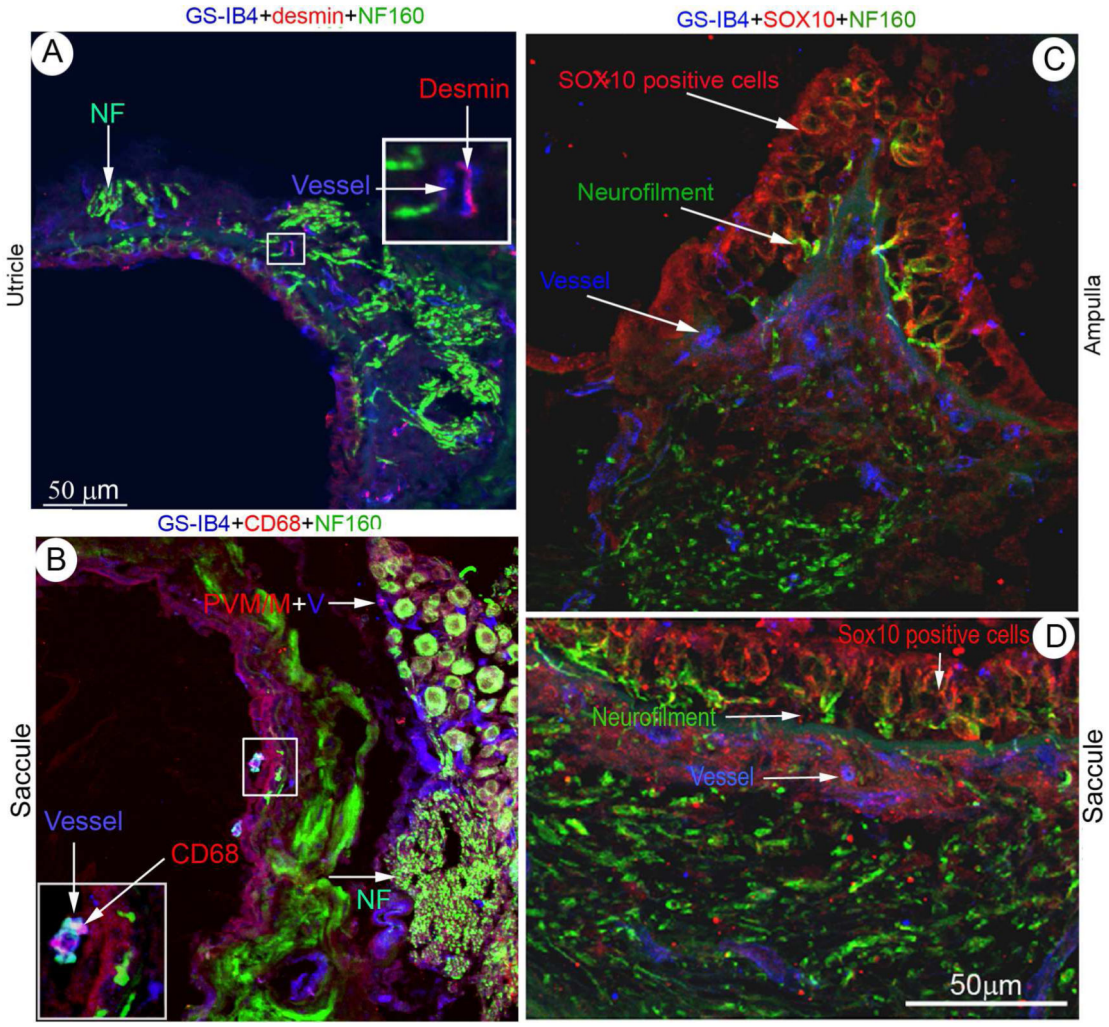

Figure 3.

Neurons in the end organs of the vestibular system do not express the PC marker protein desmin or the PVM/M marker protein CD68. SOX10 is naturally expressed in the vestibular system, but the SOX10 positive cells are not found surrounding capillaries (blue, arrow). (A) A representative confocal maximum projection image shows the fluorescence signal of the PC marker protein desmin (red, arrow) does not overlap the fluorescence signal of NF-160 (green, arrow), a neuron marker protein. (B) A representative confocal maximum projection image shows the signal of the PVM/M marker protein CD68 (red, arrow) does not overlap the fluorescence signal of NF-160 (green, arrow), a neuron marker protein. (C and D) Triple labeling of the ampulla and utricle with antibodies for SOX10 (red, arrow), NF-160 (green, arrow), and GS-IB4 (blue, arrow), show that while SOX10 is naturally expressed in the system, the majority of SOX10 positive cells are not in the proximity of capillaries labeled with GS-IB4 (blue).

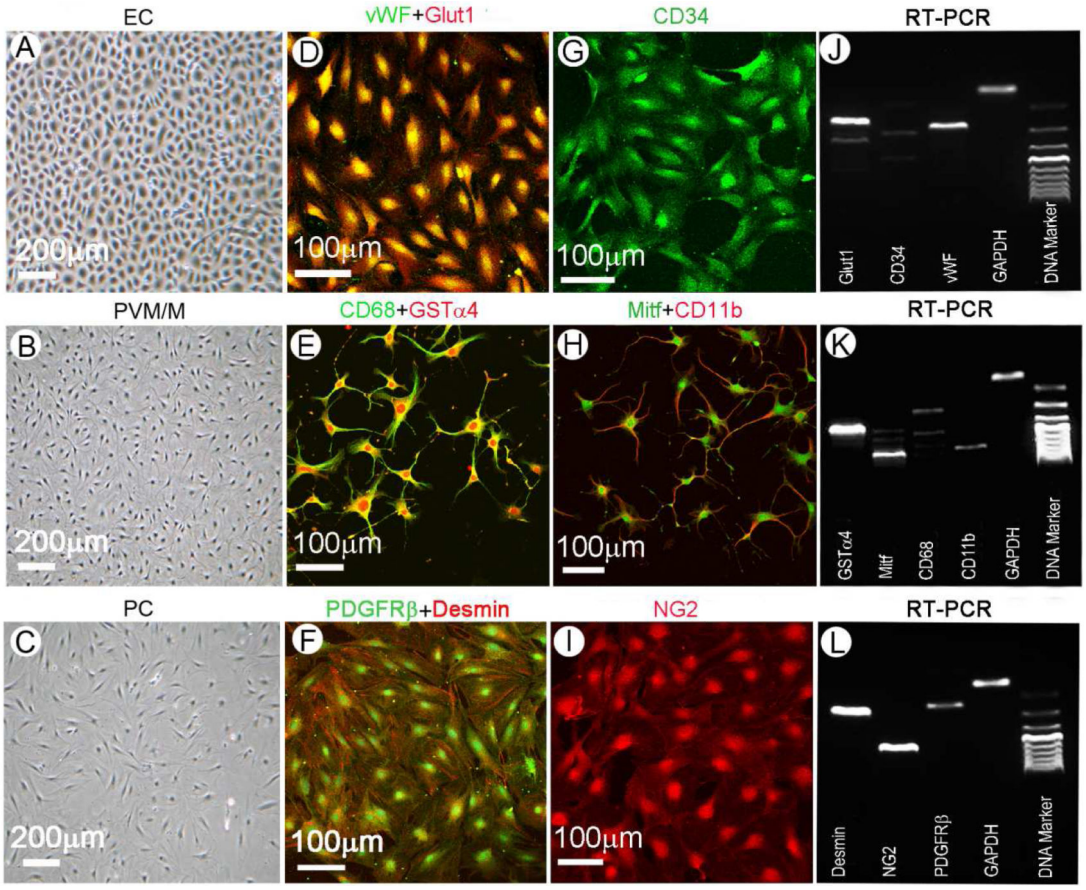

Figure 4.

Validating the phenotype of ECs, PVM/Ms, and PCs. (A-C) are DIC images of cultured ECs, PVM/Ms, and PCs at day 5 of the third passage. (D-I) show ECs labeled for (vWF, green) and Glut1 (red), CD34 (green); PVM/Ms labeled for CD68 (green) and GSTα4 (red), Mitf (green), and CD11b (red); and PCs labeled for desmin (red), PDGFRβ (green), NG2 (red). (J-L) show the RT-PCR gene analysis for each cell line.

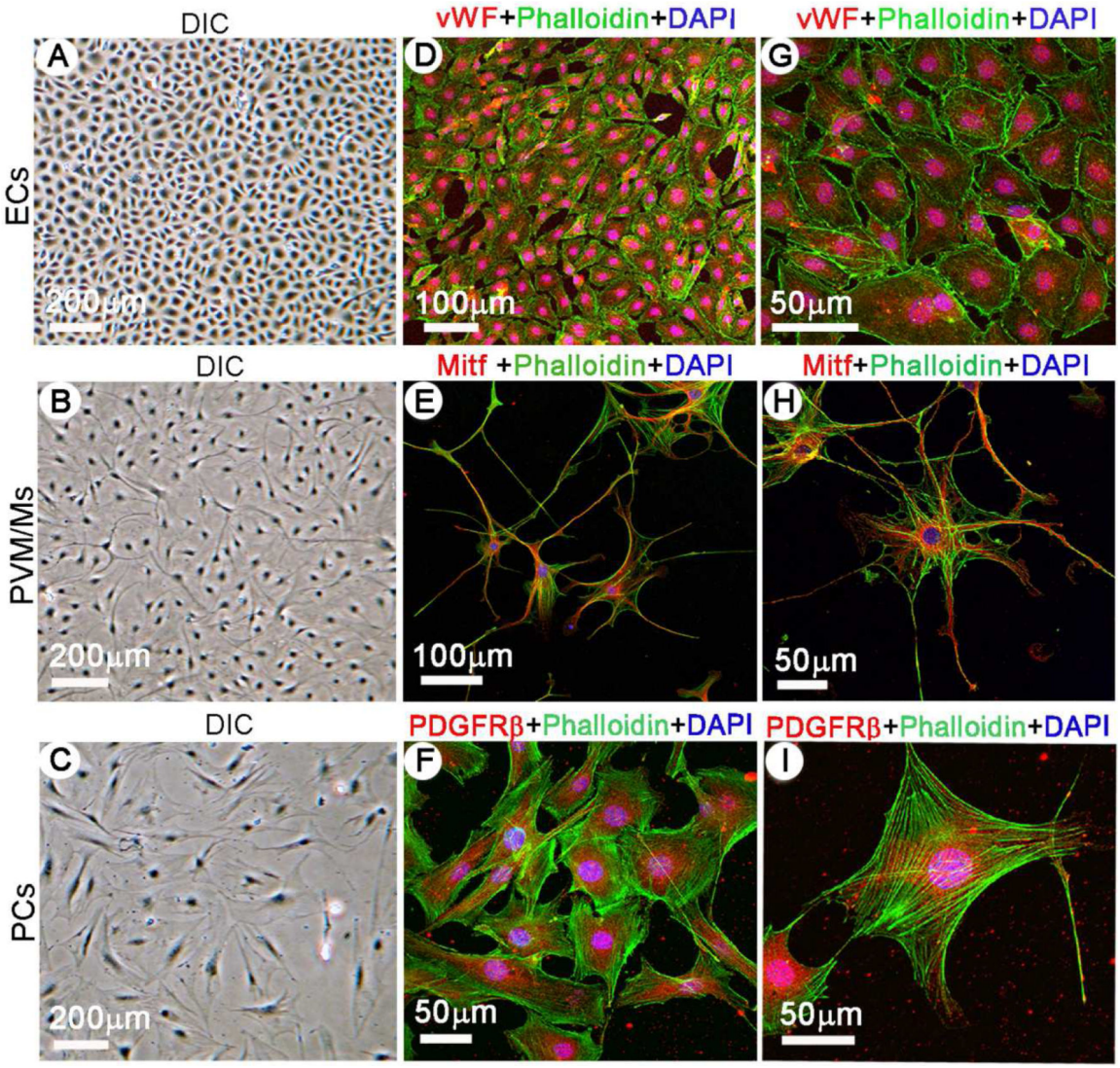

Figure 5.

Morphological validation of cell lines. (A-C) shows DIC images of the purified cell lines after FACS. (D-F) ECs are labeled for von Willebrand Factor (vWF, red), phalloidin (green), and nuclei (blue); PVMs for Mitf (red), phalloidin (green), and nuclei (blue); and PCs for PDGFRβ (red), phalloidin (green), and nuclei (blue) (G-I). ECs, PVM/Ms, and PCs are shown under high magnification with the same immunostaining.

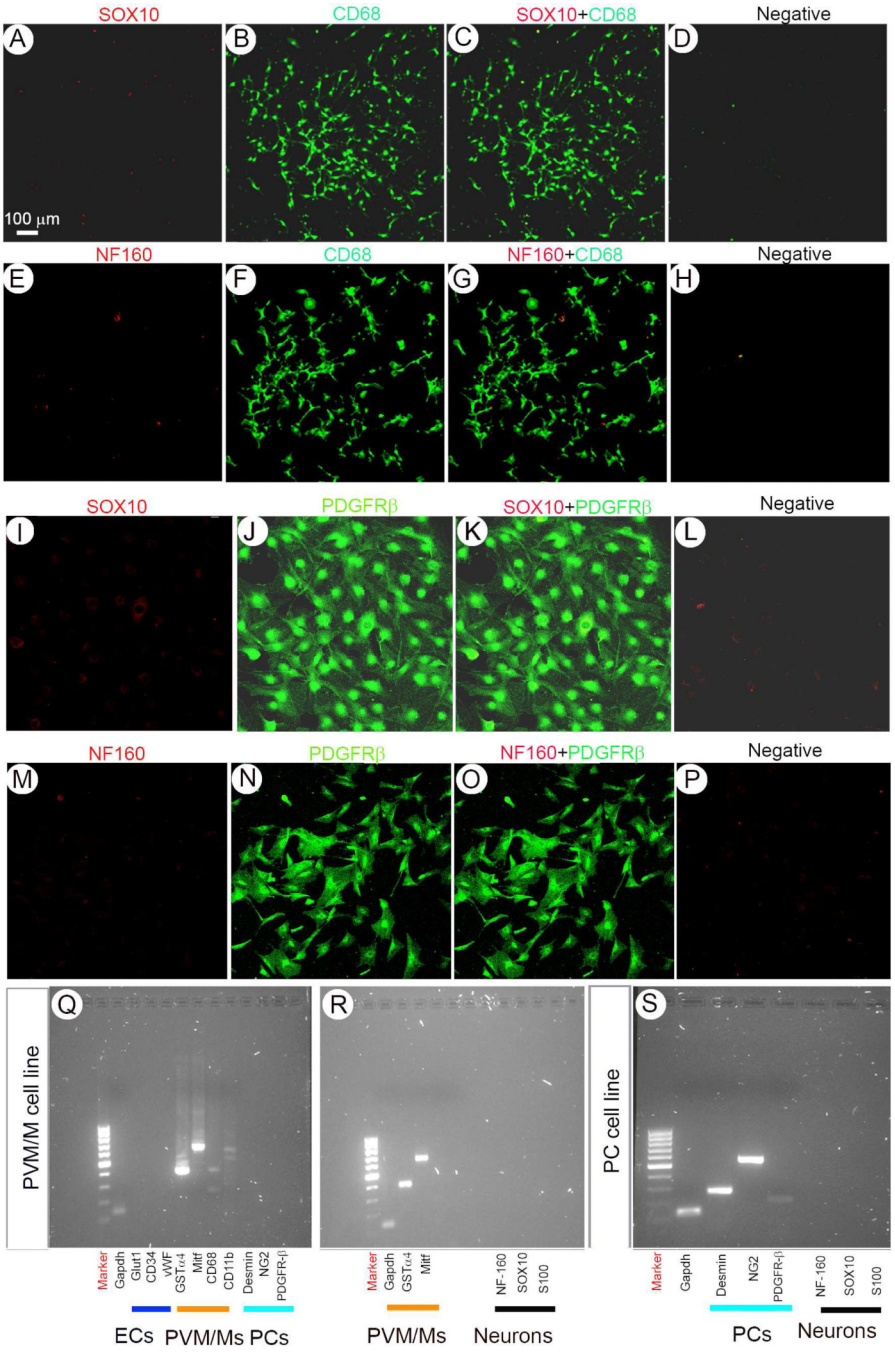

Figure 6.

The PC and PVM/M cell line verification. (A-H) show that CD68 positive PVM/Ms are negative for Schwann cell marker protein SOX10 (A-D) and they are also negative for the neuron marker protein NF-160 (E-H). (I-P) show that PDGFRβ positive PC cells are negative for both SOX 10 (I-L) and NF-160 (M-P). (Q-S)The RT-PCR multiple gene analysis for the PVM/M (M and N) and PC cell line (O) further confirms the PC or PVM/M cell line is free of neuronal cell contamination.

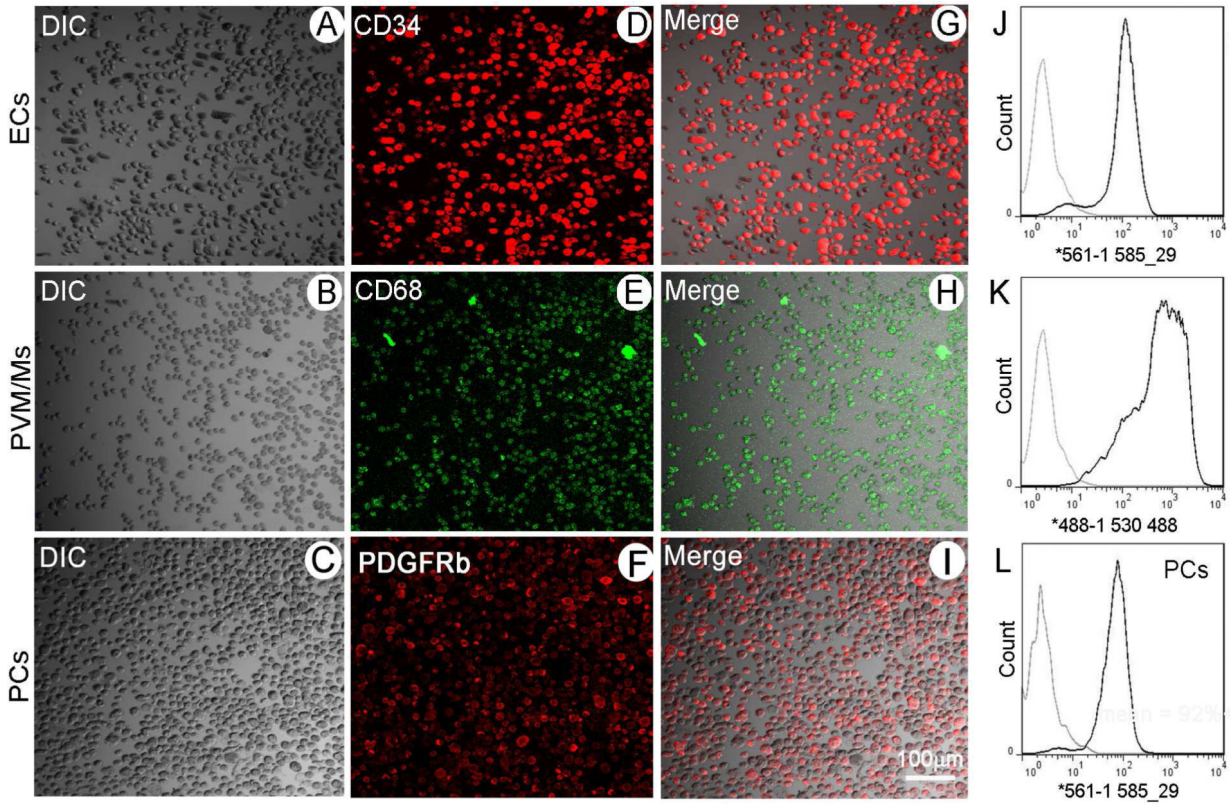

Figure 7.

DIC images of the detached cell lines (third passage at day 5) before FACS (A-C). FACS was used to assess cell purity and validate phenotype. (D-F) Merged DIC and fluorescence images of the sorted cells are shown (G-I). FACS results validate cell purity. The purity of each cell line is >90% (J-L).

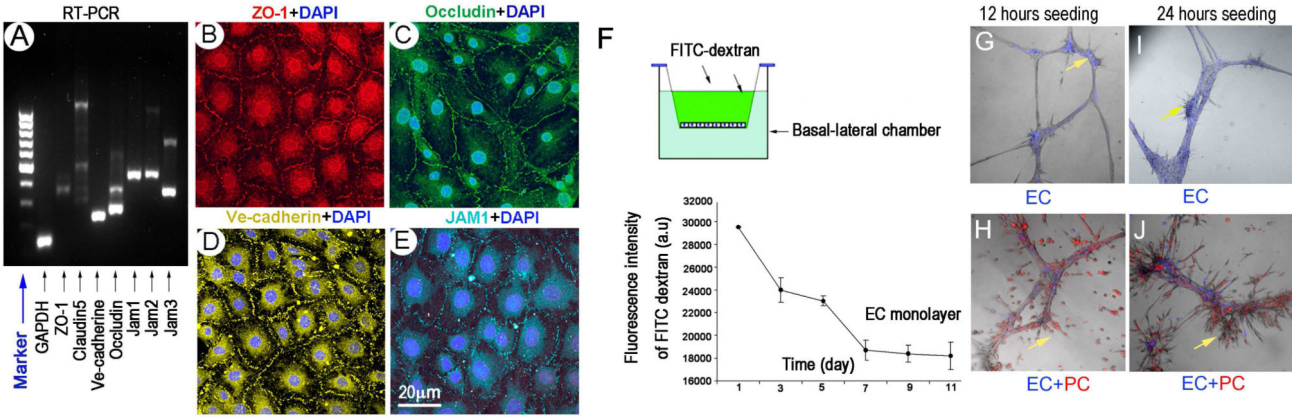

Figure 8.

Functionality of the endothelial cell monolayer and PC/EC interaction in angiogenesis. (A) RT-PCR gene analysis of tight junction associated proteins. (B-E) The endothelial cells are labeled for tight junction protein ZO-1 (red, B), occludin (green, C), Ve-cadherin (yellow, D), JAM1 (light blue, E), and nuclei (blue). (F) FITC-dextran fluorescence intensity is shown at different time points for an established endothelial cell monolayer at day 7. (G)-(J) Mono-culture of ECs and co-culture of ECs+PCs, at 12 hours and 24 hours in a matrix gel. ECs form capillary-like tubules. PCs promote a sprouting angiogenesis of these tube structures (yellow arrows). [ECs were labeled with fluorescent dye, CellTracker^{TM} Violet, PCs were labeled with CellTracker Red].

Table 1

Antibodies applied

Antibodies	Vectors	Identification	Dilution*	Source	Specificity (reacts with)
ZO-1	Invitrogen, Camarillo, CA	Cat# 61-7300	1:25	Rabbit polyclonal	Human, Mouse
PDGFRβ	Abcam, Cambridge, MA	Cat# Ab32570	1:50	Rabbit monoclonal	Rat, Human
VE-cadherin	Abcam, Cambridge, MA	Cat# Ab33168	1:50	Rabbit polyclonal	Mouse, Human
Occludin	Abcam, Cambridge, MA	Cat# Ab31721	1:50	Rabbit polyclonal	Mouse, Rat, Human, Iig
Desmin	Abcam, Cambridge, MA	Cat# Ab32362	1:50	Rabbit monoclonal	Mouse, Rat, Guinea pig,
CD68	Abcam, Cambridge, MA	Cat# Ab53444	1:50	Rat monoclonal	Mouse
Mitf	Abcam, Cambridge, MA	Cat# Ab20663	1:50	Rabbit polyclonal	Mouse, Rat, Human
vWF	Abcam, Cambridge, MA	Cat# Ab11713	1:50	Sheep polyclonal	Mouse, Human, Pig
Glut1	Abcam, Cambridge, MA	Cat# Ab15309	1:50	Rabbit polyclonal	Rat, Human
GSTα4	Santa Cruz Biotechnology, Santa Cruz, CA	Cat# sc-241483	1:50	Goat polyclonal	Human, Mouse, Bovine, Porcine
PDGF Receptor beta	Abcam, Cambridge, MA	Cat# Ab69506	1:50	Mouse monoclonal	Mouse, Rat, Human
Junctional adhesion molecule 1	Abcam, Cambridge, MA	Cat# Ab16896	1:50	Rat monoclonal	Mouse
Alexa Fluor 488-conjugated donkey anti-goat IgG	Invitrogen, Eugene, OR	Cat# A-11055	1:100	Donkey	Goat
Alexa Fluor 633-conjugated donkey anti-sheep IgG	Invitrogen, Eugene, OR	Cat# A-21100	1:100	Donkey	Sheep
Alexa Fluor 568-conjugated goat anti-rabbit IgG	Invitrogen, Eugene, OR	Cat# A-11011	1:100	Goat	Rabbit
Alexa Fluor 488-conjugated goat anti-rabbit IgG	Invitrogen, Eugene, OR	Cat# A-11008	1:100	Goat	Rabbit
Alexa Fluor 488-conjugated goat anti-rat IgG	Invitrogen, Eugene, OR	Cat# A-11006	1:100	Goat	Rat
Alexa Fluor 568-conjugated donkey anti-rabbit IgG	Invitrogen, Eugene, OR	Cat# A10042	1:100	Donkey	Rabbit
Alexa Fluor 488-conjugated donkey anti-sheep IgG	Invitrogen, Eugene, OR	Cat# A-11015	1:100	Donkey	Sheep
Alexa Fluor 568-conjugated rabbit Anti-goat IgG	Invitrogen, Eugene, OR	Cat# A-11079	1:100	Rabbit	Goat
Alexa Fluor 488-conjugated rabbit anti-rat IgG	Invitrogen, Eugene, OR	Cat# A-21210	1:100	Rabbit	Rat
Alexa Fluor® 488 donkey anti-rabbit IgG	Abcam, Cambridge, MA	Cat# Ab150073	1:200	Donkey	Rabbit
Alexa Fluor® 568 donkey anti-rat IgG	Abcam, Cambridge, MA	Cat# Ab175475	1:200	Donkey	Rat

Antibodies	Vectors	Identification	Dilution *	Source	Specificity (reacts with)
Alexa Fluor 568-conjugated goat anti-rat IgG	Invitrogen, Eugene, OR	Cat# A-11077	1:100	Goat	Rat
CD34	Santa Cruz Biotechnology, Santa Cruz, CA	Cat# sc-9095	1:50	Rabbit polyclonal	Human, Mouse, Rat
CD11b	Abcam, Cambridge, MA	Cat# Ab8878	1:50	Rat monoclonal	Mouse, Rabbit, Human
NG2	Abcam, Cambridge, MA	Cat# Ab87471	1:50	Rabbit polyclonal	Mouse
SOX10	BiossInc, Woburn, MA	Cat# Bs-6449R	1:50	Rabbit polyclonal	Human, Mouse, Rat, Bovine
NF-160	EMDmillipore	Cat# MAB5254	1:500	Mouse monoclonal	Human, Chicken, Guinea pig, Mouse, Rabbit

* dilution with 1% BSA–PBS

Table 2

Primers applied

Gene	Primer	Oligonucleotide sequence	Tm(°C)	Size
GAPDH	F	5′-ATGTGTCCGTCGTGGATCTGA-3′	58.9	132
	R	5′-AGACAACCTGGTCCTCAGTGT-3′	58	
NG2	F	5′-CAGGCCGGTCGGGTGACCTA-3′	63.9	535
	R	5′-GGGCCACGTGGAAGACACGG-3′	63.4	
PDGFRβ	F	5′-ACCTGCAGAGACCTCAAAAGTAGGT-3′	59.6	227
	R	5′-ACCACGGTGACCTCCTGCGA-3′	63.5	
Desmin	F	5′-AGCCAGCGCGTGTCCTCCTA-3′	63.5	264
	R	5′-AGCGTCGGCCAGGGAGAAGT-3′	63.6	
vWF	F	5′-ACAGACGCCATCTCCAGATTCA-3′	58.2	272
	R	5′-TGTTCATCAAATGGTGGGCAGC-3′	58.5	
Glut1	F	5′-GCTGTGCTTATGGGCTTCTC-3′	56.2	245
	R	5′-AGAGGCCACAAGTCTGCATT-3′	56.9	
CD34	F	5′-GGGAGCCACCAGAGCTATTC-3′	57.5	300
	R	5′-CACCACATGTTGTCTTGCTGA-3′	55.7	
CD11b	F	5′-GCTGCGAAGATCCTAGTTGT-3′	54.7	609
	R	5′-GCTGCCCTTGATGCTAGTGT-3′	57.7	
CD68	F	5′- AGCACAGCCAGCCCTACGAC-3′	62.2	464
	R	5′-AATGAGAGAGACAGGTGGGG-3′	56.1	
Mitf	F	5′- GGGAGTCATGCAGTCCGAAT-3′	57.2	649
	R	5′-CGTGTTCATACCTGGGCACT-3′	57.3	
GSTα4	F	5′-GCTGCGGCTGGAGTGGAGTTTG-3′	63.1	399
	R	5′-TGCCCAACTGAGCTGGTTGCC-3′	63.0	
ZO-1	F	5′- ACCATGCCTAAAGCTGTCCC-3′	57.5	354
	R	5′-CCAACCGTCAGGAGTCATGG-3	57.6	
Claudin5	F	5′- GAGTTCAGCTTCCCGGTCAA-3′	57.2	451
	R	5′- TGCCCTTTCAGGTTAGCAGG-3′	57.4	
Occludin	F	5′- CCTCCAATGGCAAAGTGAAT-3′	53.3	251
	R	5′- CTCCCCACCTGTCGTGTAGT-3′	58.6	
Ve-cadherin	F	5′- ATTGGCCTGTGTTTTCGCAC-3′	60.0	223
	R	5′- GCCTGTTTCTCTCGGTCCAA-3′	60.0	
Jam1	F	5′- AGCCAGATCACAGCTCCCTA-3′	57.7	421
	R	5′- TCTGGGCCTGGCAGTAGTAT-3′	57.8	
Jam2	F	5′- ACGCCCTCCCCTCAACCCTC-3′	64.2	421
	R	5′- TTACAAGCCAAAATAGCCTC-3′	50.4	
Jam3	F	5′- TGACAACAAGATTCAAGGAG-3′	50.0	332
	R	5′-GGAACCTGGGATTGGCTCTG-3′	58.0	
S100	F	5′-TGAGAGTGCTCATGGAACGG-3′	57.0	266

Gene	Primer	Oligonucleotide sequence	Tm(°C)	Size
	R	5′-aTTCCTCAAGTGACCCCGTG-3′	57.1	
NF-160	F	5′-TCTGGCTCTTTGATGCCCAG -3′	57.5	221
	R	5′-CGGGAAGGCTCAGAGTGTTT -3′	57.3	
SOX10	F	5′-CGCCTACACTTCCCTCAGTC-3′	57.3	274
	R	5′-GCCCCTCTAAGGTCGGGATA-3′	58.1	